

University of Groningen

Bottom-up and top-down forces in a tropical intertidal ecosystem

de Fouw, Jimmy

IMPORTANT NOTE: You are advised to consult the publisher's version (publisher's PDF) if you wish to cite from it. Please check the document version below.

Document Version

Publisher's PDF, also known as Version of record

Publication date:
2016

[Link to publication in University of Groningen/UMCG research database](#)

Citation for published version (APA):

de Fouw, J. (2016). *Bottom-up and top-down forces in a tropical intertidal ecosystem: The interplay between seagrasses, bivalves and birds*. [Thesis fully internal (DIV), University of Groningen]. Rijksuniversiteit Groningen.

Copyright

Other than for strictly personal use, it is not permitted to download or to forward/distribute the text or part of it without the consent of the author(s) and/or copyright holder(s), unless the work is under an open content license (like Creative Commons).

The publication may also be distributed here under the terms of Article 25fa of the Dutch Copyright Act, indicated by the "Taverne" license. More information can be found on the University of Groningen website: <https://www.rug.nl/library/open-access/self-archiving-pure/taverne-amendment>.

Take-down policy

If you believe that this document breaches copyright please contact us providing details, and we will remove access to the work immediately and investigate your claim.

Downloaded from the University of Groningen/UMCG research database (Pure): <http://www.rug.nl/research/portal>. For technical reasons the number of authors shown on this cover page is limited to 10 maximum.



A mutualistic feedback enhances the stability of tropical intertidal seagrass beds

Jimmy de Fouw, Tjisse van der Heide, Jim van Belzen, Laura L. Govers,
Mohamed Ahmed Sidi Cheikh, Han Oloff, Johan van de Koppel
and Jan A. van Gils

ABSTRACT

It is increasingly realized that mutualistic interactions are vital to foundation species in a wide range of ecosystems including coral reefs, seagrass beds and on plant-pollinator networks. Because such mutualisms by their very nature generate a positive feedback between the species involved, subtle environmental impacts on one of the species involved may trigger mutualism breakdown, leading to ecosystem regime shifts. Using an empirically parameterized differential equation model, we explore the importance of a mutualism between seagrass and lucinid bivalves with endosymbiotic sulfide-oxidizing chemoautotrophic gill bacteria in a tropical intertidal ecosystem. This system is characterized by rapid cyclic collapse-and-recovery dynamics by alleviating sulfide toxicity caused by organic matter accumulation within seagrass beds. Model simulations predict that the seagrass-lucinid-chemoautotroph mutualism stabilize this ecosystem. However, a minor increase in seagrass mortality above natural levels due to enhanced desiccation stress, can also trigger mutualism breakdown by pushing the system beyond a critical threshold. This generates slow-fast cycles that are characterized by long-term persistent states of bare and seagrass-dominated, with rapid transitions in between. Model predictions were consistent with remote sensing analyses combined with potential analyses that suggest feedback-mediated state shifts induced by desiccation. Overall, our combined theoretical and empirical results underline the importance of mutualistic feedbacks for stability in this ecosystem, but also reveal an important drawback as small environmental changes may trigger dramatic shifts. We therefore suggest that mutualisms should be considered as important, global targets for marine conservation and restoration of seagrass beds.

INTRODUCTION

It is increasingly realized that mutualisms form vital interactions sustaining high biodiversity in ecosystems, as many organisms are directly involved in networks of mutually beneficial interactions, such as coral reefs, seagrass beds and plant-pollinator networks (Stanley 2006, Kiers et al. 2010, van der Heide et al. 2012b, Stanley 2014). More than 90% of all tropical forest plants depend on mutualistic pollinator and/or seed dispersal interactions for reproduction (Terborgh et al. 2008, Terborgh and Estes 2010), and about 80% of all land plants are involved in mutualistic mycorrhiza-root partnerships (Smith and Read 1997). Mutualisms are particularly pervasive in coral reefs, salt marshes, mangroves, seagrass beds and deep-sea hydrothermal vents, marine ecosystems in which the ecosystem-structuring foundation species are dependent on these interactions (Bertness 1984, Ellison et al. 1996, Stewart et al. 2005, Hoegh-Guldberg et al. 2007, van der Heide et al. 2012b). Thus, such mutualisms do not only affect the species directly involved but can also have a major impact on ecosystem functioning and stability.

Although mutualism can increase the environmental range limits of the species involved, e.g., by improving stress tolerance of species (Stanley 2006, Afkhami et al. 2014, Angelini et al. 2015), recent studies also suggest an important potential unavoidable downside: because mutualistic interactions by their very nature generate a positive feedback mechanism between the species involved (Kiers et al. 2010, Lever et al. 2014), disruption of this feedback due a negative impact on one of the component species may lead to sudden shifts in ecosystem states (Scheffer et al. 2001, van der Heide et al. 2007, van Nes et al. 2007). Minor environmental changes (e.g. increase in temperature or nutrients) may potentially cause mutualism breakdown, resulting in habitat degradation (Tylianakis et al. 2008, Kiers et al. 2010, chapter 3). For example, small climate change-related phenological shifts between plants and their pollinators can cause a mismatch between mutualistic partners (Burkle et al. 2013), and in coral reef mutualisms, subtle temperature increases have been suggested to cause ‘coral bleaching events’ (Loya et al. 2001, Hoegh-Guldberg et al. 2007). Yet, even though mutualism breakdown is likely to become more common in ecosystems in the face of global change, the mechanistic insights in the role of mutualisms in systems highly depending on them remain unclear.

Here, we explore the stability of a previously documented facultative mutualism between seagrasses and lucinid bivalves with endosymbiotic sulfide-oxidizing gill bacteria for ecosystem stability. By trapping suspended particles from the water layer and stabilizing sediments, seagrasses facilitate their own growth by improving water clarity (Folmer et al. 2012, Fourqurean et al. 2012, Hansen and Reidenbach 2012). As a consequence, however, seagrass beds also create a negative feedback, because the accumulated organic matter in the sediment is decomposed anaerobically by sulfate-reducing bacteria that produce toxic sulfide as a metabolic end-product (van der Heide et al. 2012b, Lamers et al. 2013). This is where the mutualism becomes important: previous work in our study system showed that seagrasses create a positive feedback by engaging in a mutualistic interaction with lucinid bivalves and their sulfide-oxidizing, gill-inhabiting bacteria to

reduce sulfide stress. In turn, the bivalves and their endosymbionts not only profit from sulfide that is indirectly provided by seagrasses due to organic matter trapping, but also from oxygen released by seagrass roots (van der Heide et al. 2012b, Lamers et al. 2013, chapter 2 & 3). Lucinid bivalves are found in high densities in the rhizosphere of seagrasses meadows, especially in the tropics where sulfide production is generally high (van der Heide et al. 2012b, Stanley 2014).

In our study system, the tropical marine intertidal flats of Banc d'Arguin in Mauritania (West Africa), a sudden seagrass die-off event occurred in 2011 in which low-tide drought stress triggered the failure of the facultative mutualism (chapter 3), possibly after a period of strong sedimentation. Our earlier work suggests a feedback-mediated shift due to environmental stress; a hypothesis in need of further investigation. We constructed a parametrized differential equation model to (1) investigate the importance of the mutualistic interaction for seagrass ecosystem stability, and (2) test how environmental stress – low-tide desiccation stress in our case – affects ecosystem resilience. We started by analysing how our model system behaves with and without the facultative mutualistic feedback. Second, to investigate whether increases in environmental stress (e.g. drought) could lead to unstable dynamics and ecosystem collapse, we analysed the stability of the model over a range of seagrass mortality settings, which we used as a proxy for low-tide desiccation stress. Finally, we used a potential analysis – a method for detecting feedback-mediated shifts – on both model simulation results and remote sensing satellite data seagrass (NDVI) to link our theoretical results to empirical observations.

METHODS

Study system

This study was carried out in the intertidal area of Parc National du Banc d'Arguin (PNBA) in Mauritania (19°52.42'N, 16°18.50'W). The area covers around 500 km² of mudflat dominated by seagrass *Zostera noltii* (Wolff et al. 1993). Here, high densities (over 3700 ind. m⁻²) of the lucinid bivalve *Loripes lucinalis* inhabit silty, organic matter-rich sediment (up to 1-m thick) accumulated between the seagrass roots (van der Heide et al. 2012b, van Gils et al. 2013).

Model description

We developed a minimal differential equation model to investigate the importance of the mutualistic feedback between *Zostera* and *Loripes*, and the potential consequences of enhanced environmental stress for ecosystem stability. The changes in seagrass biomass are described as follows:

$$\frac{dZ}{dt} = r \left(1 - \frac{Z}{Z_{max}} \right) Z - f(mZ) \quad \text{eq1}$$

where Z is the seagrass shoot density (shoots m⁻²), r is the seagrass maximum net growth

rate (day^{-1}), Z_{max} is the carrying capacity (shoots m^{-2}), and $f(mZ)$ is a function describing seagrass mortality:

$$f(mZ) = m_s \cdot \frac{S^n}{S^n + H_s^n} \cdot Z + m_n \cdot Z \quad \text{eq2}$$

With m_s as the maximum mortality rate (day^{-1}) due to sulfide toxicity and m_n as the natural seagrass mortality (day^{-1}). Sulfide toxicity is described by a sigmoid Hill-curve (Hill 1910) – an often used function to describe toxicity in organisms – with S as pore water sulfide concentration ($\mu\text{mol L}^{-1}$), the H_s as the half-saturation constant ($\mu\text{mol L}^{-1}$), and n as a dimensionless exponent determining the slope of the curve. Changes in sediment pore water sulfide concentrations are described according to the following differential equation:

$$\frac{dS}{dt} = Com \cdot OM - C_s \cdot L \cdot S - e_s \cdot S \quad \text{eq3}$$

OM describes the amount of sediment organic matter (%), Com is a conversion factor ($\mu\text{mol L}^{-1} \%^{-1} \text{day}^{-1}$) relating organic matter decay to sulfide production, C_s is a conversion factor ($\text{m}^2 \text{ind.}^{-1} \text{day}^{-1}$) relating sulfide loss to consumption by L *Loripes* (ind. m^{-2}), and e_s (day^{-1}) describes loss of S due to chemical oxidation and diffusion to the water layer (Lamers et al. 2013). For simplicity, we assume that organic matter finds its origin mainly from seagrass detritus in our pristine system and its dynamics are described by a third differential equation:

$$\frac{dOM}{dt} = C_z \cdot f(mZ) - e_m \cdot OM \quad \text{eq4}$$

where C_z is the conversion factor ($\% \text{m}^2 \text{shoots}^{-1}$) to convert dead seagrass biomass (sh m^{-2}) to % and e_m (day^{-1}) is the loss of organic matter due to decomposition and export. Finally, *Loripes* bivalve growth is described by:

$$\frac{dL}{dt} = r_L \left(\frac{Z}{Z_{max}} \right) \left(1 - \frac{L}{L_{max}} \right) - m_L \cdot L \quad \text{eq5}$$

where L is the *Loripes* density (ind. m^{-2}) that is linearly dependent on seagrass biomass (Z), r_L is the growth rate ($\text{ind. m}^{-2} \text{day}^{-1}$), L_{max} is the carrying capacity for *Loripes*, and m_L the natural mortality of *Loripes* (day^{-1}). Note that *Loripes* spawns in the water column and growth in *Loripes* numbers is therefore independent from the number of *Loripes* already present (see for example van der Meer et al. 2001)

Model analysis

We first plotted model time plots at default settings (Table 4.1) without ($dL/dt = 0$) and with the mutualistic feedback, respectively. Next, we performed a bifurcation analysis in which we analysed the stability of the model for both scenarios over a wide range of settings of the parameter m_n , which we used as a proxy for desiccation stress. This parame-

ter was increased from 0 to 0.35 day⁻¹ in 150 steps, and the analysis was also performed backwards to detect possible alternative equilibria in the model. Model analysis was conducted with GRIND for MATLAB.

NDVI analysis and bimodality

We calculated the Normalized Difference Vegetation Index (NDVI) as a proxy for seagrass cover to empirically study seagrass distribution over the mudflat elevation gradient at Banc d'Arguin. NDVI was calculated from Landsat 5 and 8 satellite images taken at low tide at the end of summer in the warmest months (Augustus-October) in 2007, 2009, 2011 and 2013 (Appendix table A4.1). NDVI was calculated from the near-infrared (NIR) and red (RED) spectral bands: (NIR-RED)/(NIR+RED). To be able to compare NDVI images, they were first standardized them by converting the digital numbers of the spectral bands to top-of-atmosphere reflectance. Next, we empirically cross-calibrated reflectance (2009 Landsat image served as baseline), using a linear model fitted to random common ground targets with low and high reflectance (ocean and desert respectively)

Table 4.1 State and parameter values of the models and functions.

Parameters/state variable	Description (unit)	Default value	ref-value
Z	seagrass shoots shoots (m ²)	-	
S	pore water sulfide concentration (μmol L ⁻¹)	-	
OM	organic matter (%)	-	
L	loripes density (ind m ²)	-	
Z_{max}	maximum seagrass density (carrying capacity) (shoots m ²)	8,000	1
r	relative growth rate seagrass (day ⁻¹)	0.35	1,2,3
m_s	maximum seagrass mortality rate by sulfide (day ⁻¹)	0.5	1,4 ^a
m_n	natural seagrass mortality rate (day ⁻¹)	0.007	2
n	Hill-curve exponent for sulfide toxicity	5	1,2,5 ^a
H_s	half rate constant for sulfide toxicity (μmol L ⁻¹)	300	1,2,5 ^a
C_{om}	conversion factor relating % OM to sulfide (μmol L ⁻¹ % ⁻¹ day ⁻¹)	0.01/ C_z	1 ^b
C_s	conversion factor relating loss of sulfide by uptake (ind ⁻¹ day ⁻¹ m ²)	0.0027	1 ^b
e_s	loss of S due to chemical oxidation and loss water layer (day ⁻¹)	0.25	1
C_z	Conversion factor for sh/m ² to OM% (%shoots ⁻¹ m ²)	1.29e ⁻⁴	1
e_m	loss of OM due decomposition and export (day ⁻¹)	0.001	1
r_L	relative growth rate <i>loripes</i> (ind day ⁻¹ m ²)	26	6 ^a
L_{max}	maximum <i>loripes</i> density (carrying capacity) (ind m ²)	4,900	7
m_L	natural <i>loripes</i> mortality rate (day ⁻¹)	0.002	6 ^a

^a value calculated from source; ^b value dived from experiment (Appendix A4); (1) this study(Appendix A4); (2) (van der Heide et al. 2012a); (3) (Peralta et al. 2000); (4) (Holmer and Bondgaard 2001); (5) (Govers et al. 2014); (6) (Ahmedou Salem et al. 2014); (7) (van der Geest 2013).

(Song et al. 2001, Teillet et al. 2006, chapter 3). After standardization, frequency distributions of NDVI were tested for bimodality (*bimodalitytest*) as a first indication of feedback-mediated dynamics, using the software program R (R Development Core Team 2014, Holzmann and Vollmer 2008).

As a next step, we constructed a digital elevation model (DEM) dataset from Landsat images taken at varying tidal levels (Appendix Table A4.2). We manually derived the contour lines of the water edge from a range of false color image composites using Landsat SWIR, NIR and Green bands and combined these images into a single map. Different scenes that were taken in different phases of the tide were used, to find contour lines of the mudflats. Absolute elevation was assigned to the contour lines by determining the elevation of each contour line relative to mean sea level using real-time kinematic differential GPS in the field using a Trimble R8 GNSS. Finally, the DEM was created within ArcGIS 10 using 3D analyst by inverse-distance interpolation of the contour lines.

Inferring stability properties from simulated and real data

We explored if seagrass responded gradually to increased environmental stress or displays sudden shifts. If seagrass changes gradually in response to enhanced desiccation stress over the elevation gradient, the frequency distribution of seagrass cover should be unimodal, whereas feedback-mediated shifts between two states would typically result in a bimodal distribution frequency (Hirota et al. 2011, Dakos et al. 2013, chapter 3). To examine the importance of possible feedbacks in our study system, we used potential analysis, a statistical method to detect alternative states or ‘basins of attraction’ along an environmental stress gradient (Livina et al. 2010, Hirota et al. 2011, Scheffer et al. 2012). Potential analysis is based on the fact that, if distinct ecosystem states exist due to the presence of strong internal feedbacks, transitions between these feedback-stabilized states or ‘attractors’ will occur rapidly because intermediate states are inherently unstable. Note that we do not necessarily define attractors as ‘classic’ alternative stable states here because there may be other, feedback-mediated dynamics (e.g. slow-fast cycles – see discussion) that can yield similar results in the potential analysis (see results and discussion). By applying the potential analysis to both model and field data, we link our simulation results to the field situation and investigate whether the mutualism is indeed an important driver of seagrass dynamics in our study system.

Model data were prepared by simulating seagrass cover (Z_{max}) was simulated over 61 steps (step size: 0.0025 day^{-1}) of mortality m_n (0–0.15). After stabilization of 200 years, the model was ran for another 50 years with the model state being saved at the end of each year. To obtain simulation data for empirically relevant stochastic noise, 625 models were run in parallel with varying levels of carrying capacity Z_{max} obtained from a stochastic noise function with a variance ($\sigma = 0.15$) that was estimated from the NDVI data.

Field data were prepared by calibrating all 17672 NDVI values of each map allocated in 9 elevation classes of 0.1 m from –0.6 to 0.3 meter relative to mean sea level, based on the digital elevation map (DEM). Within each elevation class NDVI values were divided in bins of size $h = 1.06 \times s \times n^{-1/5}$ (s = standard deviation of z and n = number of obser-

vations/pixels) to get sufficient observations per bin to estimate the probability density function per elevation class.

Following e.g. Livina and Lenton (2007) we assumed that the variation in the simulated and observed seagrass cover are the result of underlying feedbacks and stochastic processes, which in general terms can be described as: $dz = -U'(z)dt + \sigma dW$. The first term describes the deterministic dynamics of the system, in which $U(z)$ is the potential (attractor) as the result of the feedback in the system. The second term describes the stochastic component, in which σ is the noise level and dW a Gaussian noise term. Here, the variable z denotes simulated seagrass biomass or NDVI. As we are interested in feedback-mediated bimodality in z the probability density function P_d was estimated for each elevation class using a standard Gaussian kernel estimator (with *ksdensity* function in MATLAB). The bimodality in the potential function $U = -\log(P_d)$ in a mortality or elevation class is an indication of multiple states and the local minima and maxima of U correspond to stable and unstable attractors, respectively (Scheffer et al. 2012, Dakos et al. 2013). The low- and high frequencies in seagrass biomass or NDVI were identified in automated way with the *peaksearch* function in MATLAB.

RESULTS

Model simulations

Model simulations without the mutualism at default settings (Table 4.1) predict that seagrass is inherently unstable. Seagrass peaks at shoot densities around 50% of potential carrying capacity Z_{max} , after which it quickly collapses. This is because seagrass creates a negative feedback on its own net growth, in which organic matter accumulation results in enhanced sulfide production and toxicity over time, causing the system to collapse. Following the seagrass collapse, excessive organic matter is exported from the system, in turn allowing seagrass to recolonize once sulfide levels drop below a value of about 200 $\mu\text{mol L}^{-1}$, yielding cyclic collapse-and-recovery behaviour (Figure 4.1A).

Incorporation of the mutualistic interaction into the model enhances the stability of the seagrass. The negative effect of seagrass on itself is buffered as toxic sulfide is now removed from the sediment by *Loripes* (Figure 4.1B). However, further examination reveals that a small increase in seagrass mortality (from $m_n = 0.007$ to $m_n = 0.011 \text{ day}^{-1}$) as a simulation of enhanced environmental stress creates a condition in which *Loripes* is not able to consume all sulfide produced. This causes sulfide to accumulate slowly to the point where it becomes toxic, triggering sudden seagrass degradation. At some point, the die-off then becomes enhanced by the disruption of the mutualistic feedback, sending the system back into cyclic collapse and recovery dynamics (Figure 4.1C).

A more thorough analysis of seagrass mortality m_n in a bifurcation analysis reveals that without mutualistic interaction the system displays limit cycles over the full parameter range to the point where the mortality rate exceeds the growth rate (Figure 4.2A). In contrast, bifurcation analysis of the model with the mutualism reveals a stable system

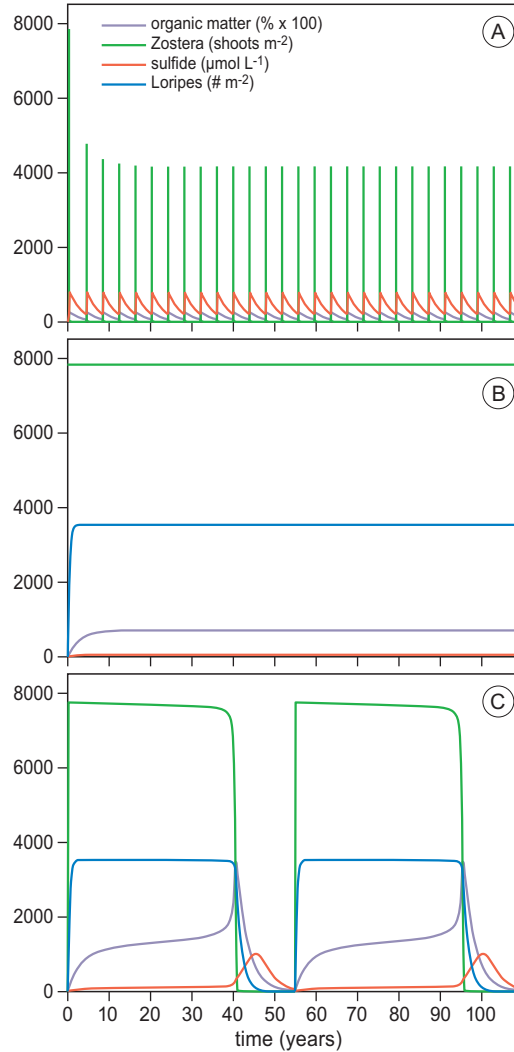


Figure 4.1 Model simulations of seagrass density Z (shoots m^{-2}), sulfide concentrations S ($\mu\text{mol L}^{-1}$), organic matter OM (%) and $Loripes$ density L (ind. m^{-2}) (A-C). (A) Model simulations at default setting without mutualistic interaction displayed short cyclic (unstable) behaviour due to a negative feedback as a result of organic matter accumulation and sulfide toxicity. (B) When adding the mutualistic interaction, any produced sulfide is removed and oscillations disappear. (C) A minor increase (from $m_n = 0.007$ to $m_n = 0.011$) of seagrass background mortality, however, causes slow-fast cycles in which the mutualism temporarily buffer against sulfide toxicity, but is not able to remove all sulfide produced, eventually causing seagrass collapse. Recovery occur when organic matter and sulfide have disappeared from the system.

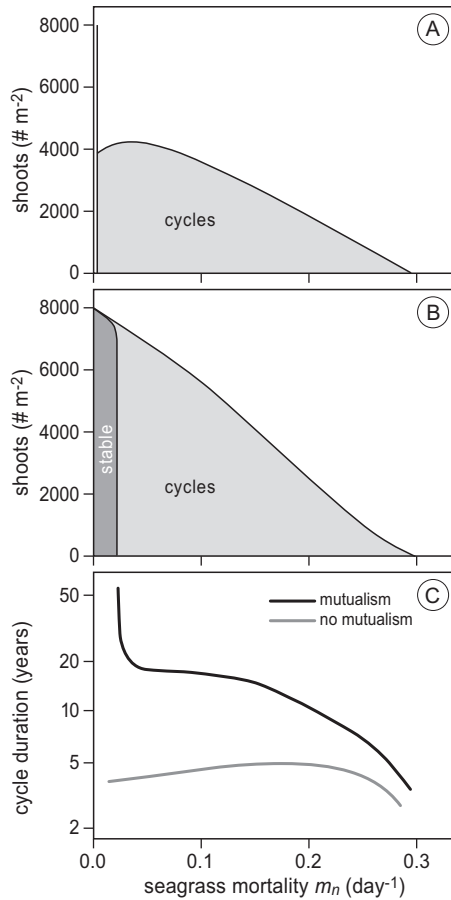


Figure 4.2 Bifurcation analysis (A) without mutualism, (B) with mutualism and (C) duration of the cycles. (A) The analysis shows that the system without mutualism the system is unstable with cyclic behaviour over the full parameter range. (B) The system with mutualism is stable at default settings, but displays cyclic behaviour after a subtle increase of mortality. (C) Although both systems display cyclic behaviour beyond $m_n = 0.011$, cycle periods of the model with mutualism are much longer compared to the model without mutualism due to the stabilizing effect of the mutualism. Grey line depicts results without mutualism, black line shows outcomes from the model with mutualism.

when seagrass mortality rates remain between 0 and 0.01 day^{-1} (Figure 4.2B). Moreover, even though the system collapses into cycles again beyond $m_n = 0.01$, the characteristics of these cycles clearly differ from those observed in the system without the mutualism: even though sulfide production eventually outpaces sulfide removal by *Loripes* when $m_n > 0.01$, collapse of the system is nevertheless dramatically postponed due the buffering effect of sulfide removal. This effect is clearly visible when comparing figures 4.1A and 4.1B, and causes much longer cycles in the model with mutualism over the full range of the bifurcation analyses (Figure 4.2C).

Potential analysis on the simulation data from the model without mutualism demonstrated a highly variable, but unimodal shoot density due to the presence of limit cycles with short periods (Figure 4.3A). Overall, low shoot density values are more abundant relative to high values due to the sharp peaks in the cycles (Figure 4.1A), causing the potential analysis to identify a single attractor at low shoot densities in the system. Very different dynamics are found in the simulation data from the model with mutualism. The potential analysis finds a single stable attractor in when mortality is low (i.e. $m_n < 0.01$ day⁻¹). Here, the mutualistic interaction keeps the system in one state with high shoot densities at carrying capacity (8000 ± 1200 shoots m⁻² (mean \pm SD)) (Figure 4.3B). However, when m_n is increased beyond 0.01 day⁻¹ and the system displays cycles (Figure 4.2B), the potential analysis identifies two main attractors: one at high and one at very low shoot densities. In contrast to the model without mutualism, the analysis identified two attractors here because the cycles stay in both a high and low state for a relatively long time compared to intermediate shoot densities due to the buffering effect of the mutualism (Figure 4.1C).

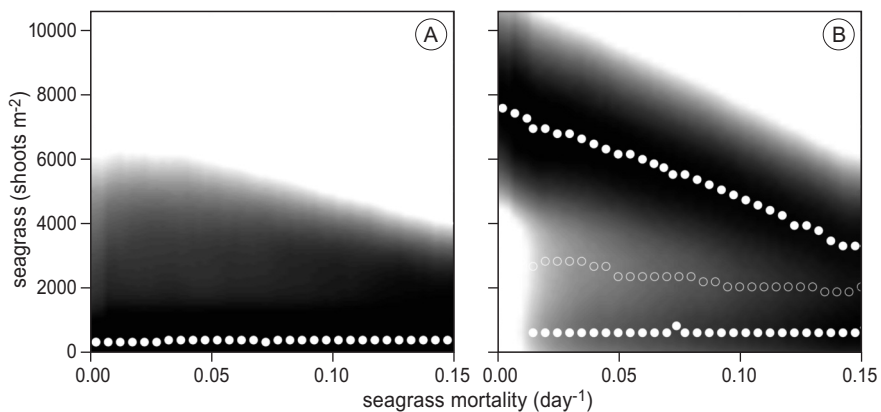


Figure 4.3 Potential analysis of the simulated seagrass data (A) without mutualism and (B) with mutualism in relation to seagrass mortality (m_n). Dark and light shades depict shoot density ranges of high and low occurrence, respectively; closed and open markers depict ‘attractors’ (peaks in occurrence) and ‘repellers’ (lows in occurrence) that are automatically identified by the analysis 0.0025 day⁻¹ mortality m_n step size.

FIELD DATA RESULTS

NDVI analysis on temporal dynamics and spatial heterogeneity of sea grass cover revealed a rather stable period in seagrass cover between 2007 and 2011 after which a 44% decline followed between 2011 and 2013 (Figure 4.4A-D) which was found to be associated with drought-induced enhanced desiccation stress and disruption of the mutualistic feedback (chapter 3). The frequency distribution of NDVI showed a significant bimodal distribution for 2011 ($P < 0.001$), but this was not detected in 2007, 2009 and 2013

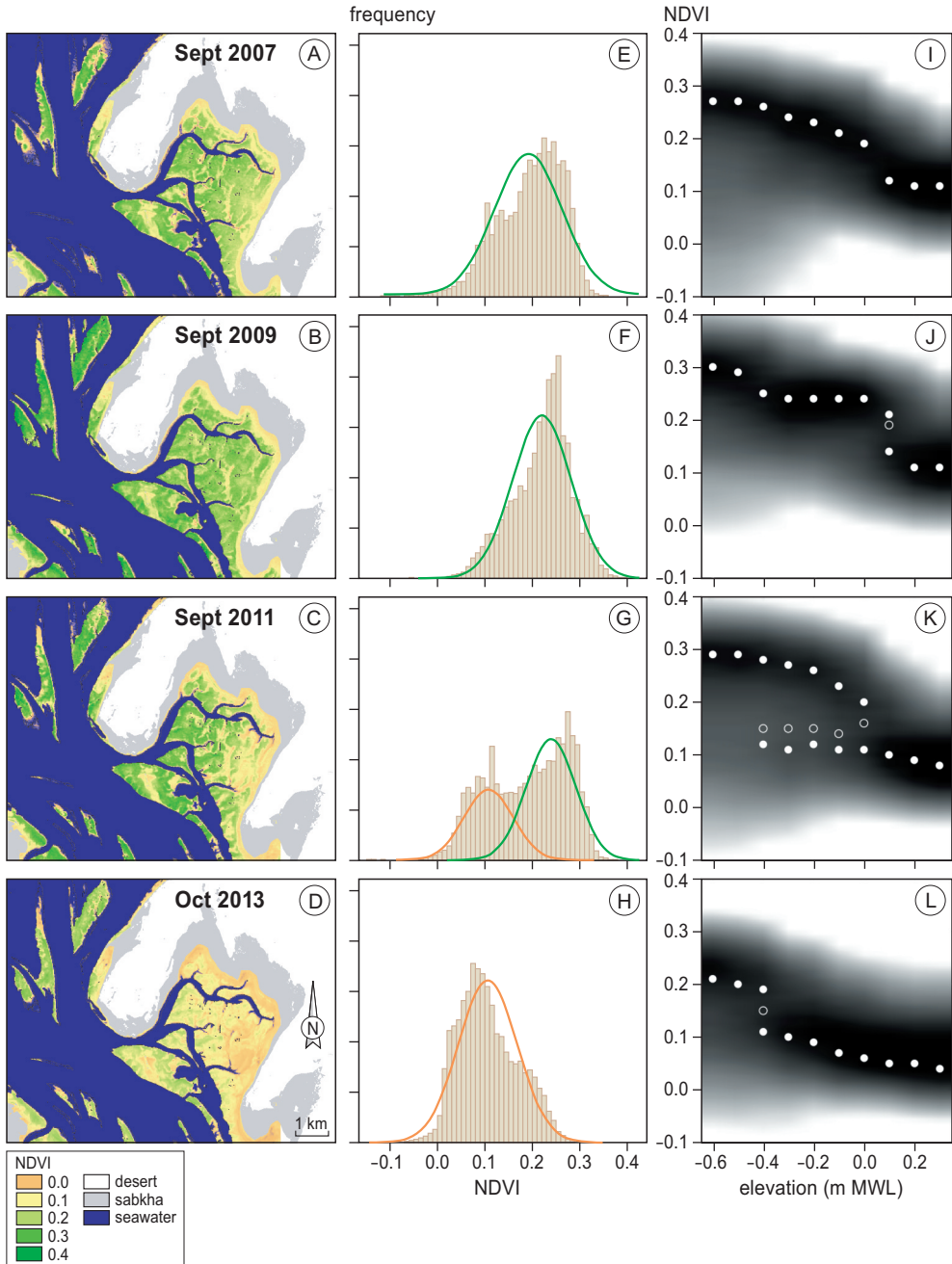


Figure 4.4 (A-D) NVDI in our study area (Banc d'Arguin, Mauritania) from 2007 to 2013 as calculated from Landsat imagery at low tide. (E-H) Frequency distribution of NDVI data and (I-L) the potential analyses of the NDVI data, dark and light shades depict NDVI ranges of high and low occurrence, respectively; closed and open markers depict 'attractors' (peaks in occurrence) and 'repellers' (lows in occurrence) that are automatically identified by the analysis per 0.1-m elevation interval. Figures A-D and I-L were adapted from (chapter 3).

($P = 0.5$) (Figure 4.4E-H). This bimodality suggests a feedback-mediated sudden shift rather than a gradual response. This was supported by the potential analysis of the NDVI data. Similar to the results from our model with mutualism at low mortality levels (i.e. where the system is stable), analyses on maps of 2007 and 2009 revealed one point of attraction that decreased with increasing elevation, suggesting that desiccation was an important factor causing lower seagrass cover in areas of higher elevation and exposure times (Figure 4.4 I-J). During the drought event in 2011, the analysis identifies two attractors at intermediate elevations (-0.4 to 0 m MWL), indicating that areas with high seagrass cover shifted to a degrading state (Figure 4.4K). Furthermore, the higher attractor decreases with increasing elevation, again indicating that seagrass cover is related to desiccation. In 2013 most areas at intermediate elevations had transitioned from a high seagrass cover state to a degraded state as only the lower attractor was stable above -0.4 m MWL (Figure 4.4L).

DISCUSSION

Mutualisms, due to their very nature, create a positive feedback between the species involved, and these feedbacks have been hypothesized to stabilize communities and ecosystems, especially if the mutualistic interaction involves a foundation species structuring the ecosystem (Stachowicz 2001). In this study, we demonstrate how a mutualism-driven positive feedback buffers a negative feedback imposed by the foundation species upon itself, thereby stabilizing the ecosystem in a seagrass-dominated state. More specifically, simulations from our empirically calibrated model predict that in absence of the mutualism, anaerobic decomposition of organic matter accumulated by seagrass itself leads to limit cycles due to excessive production of toxic sulfide. By contrast, in the presence of the seagrass-bivalve-bacteria mutualism, sulfide toxicity is alleviated because sulfide is consumed by the lucinid bivalve-bacteria consortium, thereby stabilizing the ecosystem under default conditions.

Our model analyses, however, also reveals an important inherent risk of mutualism-dependency: if the mutualism is weakened due to enhanced environmental stress – in our model simulated by enhanced natural seagrass mortality – the sulphide-buffering capacity of the mutualistic feedback can be exceeded, resulting in ecosystem collapse. Potential analyses on simulation results from the model with mutualism identified a single stable attractor at high shoot densities at default parameter settings. Here, any produced sulphide is immediately removed by the seagrass-lucinid mutualism. However, when mortality was enhanced beyond a certain threshold, a second attractor at low shoot densities was identified. In addition, the analysis predicts that seagrass shoot density for the highest attractor (i.e. seagrass-dominated state) gradually decreases with increasing mortality. These findings were very similar to results we obtained from the potential analyses on the field data. In periods with low desiccation stress (i.e. 2007 and 2009)(see for details chapter 3), only a single attractor a high NDVI was stable and gradually decreased within

increasing elevation. During the 2011-drought, however, a second low-NDVI attractor was identified, suggesting a feedback-mediated shift towards the degraded state observed in 2013. Such ecosystem dynamics following gradual environmental change or perturbations of strong positive feedbacks have been described for a wide range of ecosystems (Scheffer et al. 2001, van der Heide et al. 2007). For example, shallow lakes under excessive nutrient loading switch from clear to a turbid state (Scheffer et al. 1993) and climate change-related shifts in plant-pollinator disruptions (Potts et al. 2010, Burkle et al. 2013); the expelling of zooxanthellae by corals leading to ‘coral bleaching events’ (Loya et al. 2001, Hoegh-Guldberg et al. 2007).

In many ecosystems, strong positive feedbacks can cause alternative states (i.e. bistability), implying that through gradually changing environmental conditions or a perturbation, a critical threshold can be crossed, causing a shift to an alternative state. If conditions subsequently improve, they have to progress beyond the point of collapse, before recovery to the initial state can take place, a phenomenon called hysteresis. In seagrass meadows, such hysteresis can for instance occur at high water column ammonia loading, as ammonia toxicity can only be alleviated through joint uptake and detoxification of ammonia by ample seagrass meadows of high density (van der Heide et al. 2008, van der Heide et al. 2010b). In our study system, however, the mutualistic feedback does not appear to lead to alternative stable states dynamics, but instead causes the occurrence of so-called “slow-fast” cycles. The dynamics of our model are similar to what was advanced as a potential explanation for cyclic shifts in shallow lakes where accumulation of phosphorus creates a “time bomb-effect” due to slow internal eutrophication (van Nes et al. 2007). In our system, the mutualism initially buffers sulfide production, but excessive organic matter accumulation (the “time bomb”) by seagrass at higher background mortality (m_n) causes sulfide production to gradually increase and eventually outpace and overwhelm sulfide consumption by the mutualism, causing an abrupt shift to a bare state. Following the shift, however, organic matter is slowly exported from the system again, by erosion (the seagrass does not retain it anymore), followed by a period where seagrass can re-establish once organic matter and sulfide production drop below a certain threshold. This effectively causes slow-fast dynamics characterized by states that are persistent for long times, either seagrass or bare, with fast shifts (collapse and recovery) in between (Rinaldi and Scheffer 2000, van Nes et al. 2007, Dakos et al. 2015).

Interestingly, our model predictions reveal that such slow-fast dynamics can create patterns (i.e. bimodality) that are very similar or equal to the signature of alternative stable states in a potential analysis. So far, bimodality (multiple peaks in the frequency distribution) in potential analyses has mainly been attributed to the potential existence of multiple stable states (Hirota et al. 2011; Scheffer et al. 2012; van Nes et al. 2014). Our results, however, suggest that caution is warranted when interpreting multimodality in potential analysis or bimodal frequency distributions, as multiple types of ecosystem dynamics (albeit all typically feedback-driven) may cause similar patterns in these analyses. As there are multiple examples of ecosystems with a potential for slow-fast dynamics (Barkai and McQuaid 1988; Dakos et al. 2015; Ludwig et al. 1978; Rinaldi and Muratori 1992a;

Rinaldi and Muratori 1992b; van Nes et al. 2007), our finding stresses the need for sufficient mechanistic insights when interpreting proxies or indicators for feedback-driven dynamics (e.g. van der Heide et al. 2010a, van der Heide et al. 2012a, Weerman et al. 2012).

As current global climatic changes lead to increased average temperatures as well as an increase in the number of extreme events, it seems likely that stress events will become a more common phenomenon (IPCC 2014). This is especially the case in the tropics where high temperatures in combination with strong winds can cause desiccation events, particularly during neap tides with prolonged low tide exposure (van Lent et al. 1991, Seddon et al. 2000). Indeed, our study combined with earlier work (Seddon et al. 2000, Massa et al. 2009, chapter 3) suggests that desiccation stress is an important stressor that can initiate ecosystem degradation. For Africa predictions suggest that the average temperature will increase by 3–4°C in the next 100 years (Christensen et al. 2007, Cook and Vizy 2015). Indeed, in our study area average temperature has increased by 0.06°C per year between 1996 and 2013 ($P = 0.014$, $R^2 = 0.32$; Appendix Figure A4.3) for the hottest months (August–October, data from Nouadhibou weather station; www.tutiempo.net). Apart from temperature increase, however, there are also other climate change related effects (e.g. sea-level rise, eutrophication and siltation events) that may affect seagrass meadows (Orth et al. 2006). For example, one may expect sea-level rise to mitigate the enhanced risk of desiccation stress. Still, apart from increased mean sea level, the tidal variation around the mean will also increase (Short and Neckles 1999), potentially enhancing low-tide exposure time and desiccation stress. Also, major Sahara-born dust storms may cause excess sedimentation promoting seagrass mortality. Apart from seagrass meadows, many other coastal systems also depend on mutualisms (e.g. coral reefs, salt marches and mangroves) and have declined rapidly (Jackson et al. 2001, Waycott et al. 2009). As climate change-induced mutualism breakdown is likely to become more common in the future (Kiers et al. 2010), we suggest that a more mechanistic insight into these dynamics is required and that marine mutualisms should be considered as important conservation and restoration targets.

ACKNOWLEDGMENTS

We thank the Director and employees of the Parc National du Banc d'Arguin for supporting our work. We thank Leon P. M. Lamers and Alfons J. P. Smolders useful discussions during experimental for advice and useful discussions on field experiments for parameter estimation, and Marolijn Christiaan and Karin van der Reijden for assistance during the experiments. We thank Theunis Piersma who made helpful comments on the manuscript and D. Visser for illustrations. JdF would like thank the organisers, lectures and participants of the Consumer Resource Interactions course for fruitful discussions and comments on preliminary results. JdF and JAvG were financially supported by the personal VIDI grant 864.09.002 awarded to JAvG and TvdH by the personal VENI grant 863.12.003, both supported by the Netherlands Organisation for Scientific Research (NWO).

APPENDIX A4

Table A4.1 Landsat images used for elevation map and calculation of NDVI. Digital elevation map was based on 9 Landsat images with different tide levels. Contour lines of the water edge were manually derived from a false color image composite using Landsat SWIR, NIR and Green bands and combined into a new map.

Landsat image	sea level	time acquisition
1973-02-22 LS1MSS	-1.3	11:01:40
2001-12-18 LS7ETM	-1	11:20:55
2011-09-17 LS5TM	-0.95	11:20:31
2010-07-28 LS5TM	-0.58	11:22:29
2011-01-04 LS5TM	-0.3	11:21:58
2014-03-17 LC8	-0.4	11:32:31
2014-03-01 LC8	-0.2	11:32:40
2011-07-15 LS5TM	0.1	11:21:11
2011-06-13 LS5TM	0.2	11:21:24

Table A4.2 Landsat images used for the GIS analyses to calculate NDVI. Suitable (i.e. regarding season, low tide, haziness) Landsat images used for the GIS analyses.

Image	date	time	Mapping
Landsat 5	15-Sep-2007	11:18:58	NDVI
Landsat 5	11-Sep-2009	11:21:45	NDVI (baseline map)
Landsat 5	17-Sep-2011	11:20:31	NDVI
Landsat 8	24-Oct-2013	11:33:49	NDVI

SUPPLEMENTARY TEXT ON MODEL PARAMETER ESTIMATION

Derivation of maximum seagrass mortality due to sulfide toxicity

We derived the maximum seagrass sulfide mortality m_s using a modified version of equation 1 in which we set the Hill-response curve to 1 (see main text). We used default values derived from the literature for all other parameters (table 4.1, see main text). Next, m_s was estimated at 0.5 day^{-1} where the maximum seagrass mortality was reduced by 80% after 6 days (Holmer and Bondgaard 2001).

Mortality response of *Z. noltii* to sulfide

To estimate the toxicity effect of *Z. noltii* we parametrized the Hill-curve (equation 2, see main text) using experimental data from literature (van der Heide et al. 2012b, Govers et al. 2014)

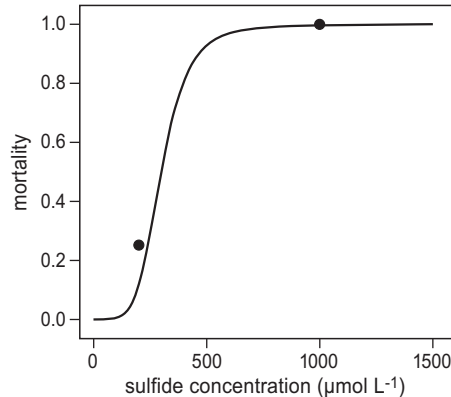


Figure A4.1 (A) Parc National du Banc d'Arguin (PNBA) in Mauritania, West-Africa with intertidal Mortality response curve of *Z. noltii* to sulfide derived from literature. At 200 µmol L⁻¹ there is a reduction of 25% and at 1000 µmol L⁻¹ there is a 100% reduction in seagrass biomass (van der Heide et al. 2012b, Govers et al. 2014).

Estimation of conversion factor C_{om} relating percentage organic matter to sulfide production

Method – To investigate sediment pore water sulfide production in seagrass meadows in our study system, we conducted a laboratory experiment in our field station at Banc d'Arguin. We measured pore water sulfide production by filling 500 ml bottles anaerobically collected sediment (including seagrass detritus) from a healthy seagrass meadow (6770 shoots m⁻² and 309.5 dry mass gram m⁻²) (J. de Fouw, L. L. Govers and T. van der Heide unpub. data). Sediment was extracted from the upper 5 cm of the seagrass sediment layer in the field by using a Teflon tube (5 mm inner diameter) connected to vacuum 500 ml bottles and connected to a vacuum pump. In the laboratory, bottles (n = 7) were wrapped in aluminium foil and incubated in water for three days at an average temperature of 26.8°C. Pore water sulfide concentrations were measured daily by collecting pore water samples in 60-ml vacuumed syringes connected to 5-cm rhizon samplers (Eijkelkamp Agrisearch Equipment, Giesbeek, the Netherlands) (van der Heide et al. 2012b) that had been inserted into the bottles through an airtight rubber seal. The total dissolved sulfide concentration in the pore water was measured immediately after sampling, in a mixture of 50% sample and 50% Sulfide Anti-Oxidation Buffer (SAOB) using an ion-specific silver-sulfide electrode (Lamers et al. 1998). In addition, we measured sediment organic matter in the upper 5 cm of the sediment in the field. Sediment samples

were taken with a small tube (10 ml), weighed immediately after collection and frozen (-10°C). Samples were freeze-dried in the laboratory, after which we determined organic matter as loss on ignition (LOI; 5 hrs at 560°C).

Result – Based on the organic matter content in the 10 ml tube we calculated the organic matter content for the top 5 cm per m^2 . The tube contained 0.704 g ml^{-1} of sediment dry mass containing 7% organic matter (OM), which is: $0.049 \text{ g organic matter ml}^{-1}$. Hence, the top 5 cm of a healthy seagrass beds contains than $2464 \text{ g organic matter m}^{-2}$ ($0.049 \times 50 \text{ L} \times 1000$). To estimate conversion factor C_{om} relating organic matter to sulfide production, organic matter was converted to shoots m^{-2} , by dividing 2464 by the biomass of a single shoot (0.045 g). This comes down to an organic matter equivalent of $54000 \text{ dead shoots m}^{-2}$. In this rich organic matter sediment sulfide concentration increased on average with $686.6 \mu\text{mol L}^{-1} \text{ day}^{-1}$. Hence, the sulfide conversion factor C_{om} was estimated at $686.6/54000 = 0.01 \mu\text{mol L}^{-1} \text{ shoots day}^{-1} \text{ m}^{-2}$.

Conversion factor C_s relating loss of sulfide by uptake

Method – To investigate the sulfide uptake by *Loripes*, we conducted an experiment in the field station at Banc d'Arguin. *Loripes* for the experiment were collected from the seagrass meadows at Abelgh Eiznaya ($19^{\circ}53.54'\text{N}$, $16^{\circ}18.85'\text{W}$). The lower 6-cm tall sections of 8 two-compartment PVC columns (diameter 8.4 cm) were filled with seawater (figure A4.2; after van der Heide et al. 2012b). These 330-ml sections contained an injection tube and were separated from their upper compartments through a porous 0.1-mm membrane. Upper compartments were filled with sieved (1-mm mesh) iron-free silver sand to prevent formation and precipitation of iron-sulfides. Next, we placed five *Loripes* ($7.44 \pm 0.58 \text{ mm}$ (mean \pm SD) per column (900 ind. m^{-2}) were added on top of the sedi-

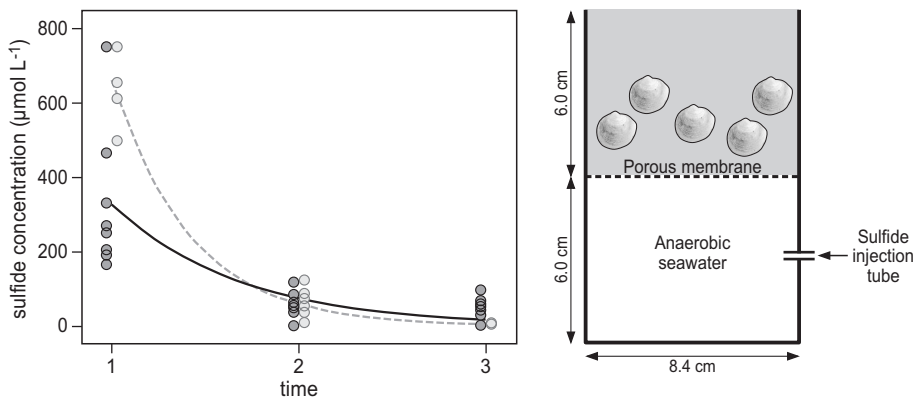


Figure A4.2 Sulfide loss by uptake of *Loripes* and schematic drawing of the setup of an experimental unit. Sulfide was injected every three days in the and allowed to diffuse from the lower compartment into the upper section through a 0.1-mm porous membrane. Parameter C_s was estimated based on injection of 500 and $1000 \mu\text{mol L}^{-1}$ sulfide at $t = 0$, black line and dashed line respectively.

ment surface, which subsequently buried themselves into the sediment. The columns were placed in plastic basins ($57.0 \times 39.0 \times 30.0$ cm) with seawater where water flow and oxygen saturation were maintained with a pump. Salinity and pH were kept constant by adding fresh water and seawater when needed (measured with a 556 Multi Parameter Sampler, Yellow Springs Instruments). Sulfide was added every third day by injecting a $100 \mu\text{mol L}^{-1}$ Na_2S solution (set at pH 7.5 with HCl) into the lower compartment, 500 and $1000 \mu\text{mol L}^{-1}$ respectively (1.5 and 3.0 ml). Prior to injection, pore water was sampled from the upper compartment using pre-inserted 5-cm rhizons and measured following the procedure above (see **Estimation of C_{om}**).

Result – Sulfide uptake by *Loripes* C_s was estimated at $-0.0027 \text{ m}^2 \text{ day}^{-1} \text{ ind}^{-1}$ using a non-linear model: $S_{ti} = S_{t0} \times e^{C_s \times L \times \text{day}}$ (Figure A4.2). Here, L is the *Loripes* density (900 ind. m^{-2}), S_{t0} is the sulfide concentration after injection, and S_{ti} is the sulfide concentration at day i - we tested 500 and $1000 \mu\text{mol L}^{-1}$ respectively (see Figure A4.2).

Loss of sulfide due to chemical oxidation and loss water layer

Apart from sulfide uptake by *Loripes* there is a constant loss of sulfide due to chemical oxidation and diffusion to the water layer. We derived this constant loss of sulfide using a modified version of equation 3 in which we assumed no sulfide uptake by *Loripes*:

$$dS/dt = C_{om} \cdot OM - e_s \cdot S$$

where S is the maximum sulfide concentration ($2,000 \mu\text{mol L}^{-1}$) in healthy seagrass with a sediment organic matter of 7% (see **Estimation of C_{om}**). Sulfide loss e_s was estimated at 0.25 day^{-1} .

Estimation of conversion factor C_z shoots to relating percentage organic matter

Organic matter is expressed in percentage therefore we need to convert $f(mZ)$, the function describing seagrass mortality, to percentage. To calculate the conversion factor C_z we assessed the maximum organic matter content in healthy seagrass, by dividing 7% organic matter by $54,000 \text{ shoots m}^{-2}$ (see details on numbers C_{om}) and was estimated at $0.129 \times 10^{-4} \mu\text{mol L}^{-1} \%^{-1} \text{ day}^{-1}$.

Loss of organic matter due decomposition and export

We assume a constant loss of organic matter e_m from the system due to decomposition and export. This parameter was derived by isolating equation 4 (see main text), assuming again a maximum sediment organic matter of 7% for a healthy seagrass bed (with an equivalent of $54,000 \text{ shoots m}^{-2}$, see calculation for C_{om}) and using only natural seagrass mortality rate m_n as a source of input. Next, daily loss of organic matter e_m was estimated to be 0.001 day^{-1} .

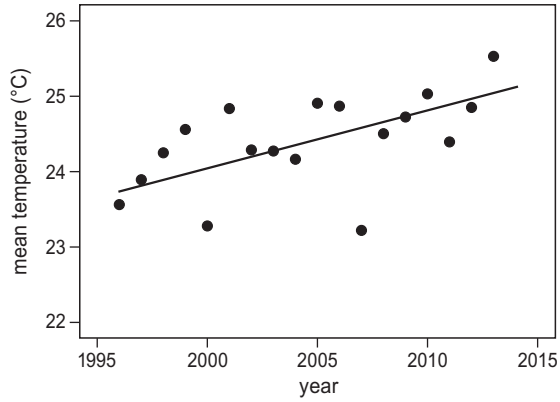
Temperature increase Mauritania 1996–2013

Figure A4.3 Average temperature in Banc d'Arguin between 1996 and 2013. Significant increase in average temperature of 0.06°C per year ($P = 0.014$, $R^2 = 0.32$) for the hottest months August-October. Data from Nouadhibou weather station: www.tutiempo.net.